Impingement of Single and Twin Turbulent Jets Through a Crossflow

J. M. M. Barata,* D. F. G. Durão,† and M. V. Heitor*
Instituto Superior Técnico, 1096 Lisbon, Portugal
and
J. J. McGuirk‡
Imperial College of Science and Technology, London, SW7 2BX England, United Kingdom

Laser-Doppler measurements of velocity characteristics of the flowfield resulting from the impingement of single and twin jets against a wall through a low-velocity crossflow are presented and discussed together with visualization of the flow. The experiments have been carried out for a velocity ratio between the jets and the crossflow of 30, for a Reynolds number based on the jet exit Re_j between 60,000 and 105,000, and for the jet exit 5 jet diameters above the ground plate. In addition, calculations based on a two-equation turbulence model are presented for the three-dimensional flow characterized by the measurements, and comparison between experimental and numerical results show that the mean flowfield is well predicted. The calculation of the turbulent field requires, however, consideration of the individual stresses.

Nomenclature

D = diameter of the jet
H = height of the crossflow channel
k = turbulence kinetic energy
Re = Reynolds number
S = distance between the jet along transversal direction
U = horizontal velocity, $U = \bar{U} + u'$
V = vertical velocity, $V = \bar{V} + v'$
X = horizontal coordinate (positive in the direction of the crossflow)
Y = vertical coordinate (positive in the direction of the jet flow)
Z = transverse coordinate (positive on the right side of crossflow duct looking upstream)

Subscripts
j = jet exit value
0 = crossflow value

I. Introduction

THE flow of single or multiple jets issuing into a crossflow is of great practical relevance in many engineering situations. Examples are the discharge of exhaust gases from a chimney into the atmosphere or of waste liquids into water, film cooling of turbine blades, and dilution jets in gas-turbine combustors. In addition, if the crossflow is confined and the jet-to-crossflow velocity ratio is high, further complexity may be introduced by jet impingement, and the most practical relevance is to the flow beneath a short takeoff/vertical landing (VSTOL) aircraft close to the ground. In this application, the lift jets interact strongly with the ground plane and with the crossflow, forming a ground vortex that wraps around the impingement regions and an upwash fountain resulting from the collision of the wall jets. These phenomena can lead to engine thrust losses following reingestion of the exhaust gases, to oscillations in the pitching and rolling moments, and to enhanced entrainment close to the ground (suckdown).

The study of impinging jets through a crossflow provides a basis for understanding the essential dynamics of these complex engineering situations. Here, detailed laser-Doppler measurements of typical single and twin jets against a wall through a low-velocity crossflow are presented because they are essential to improve understanding of the structure of the comparatively more complex practical flowfields and to allow the validation of numerical methods used to simulate those practical flows. The measurements were obtained in a water flow rig under isothermal conditions, and although they do not represent the compressibility effects and coupling of the energy equation that are present in the actual situation, they do allow the analysis of the turbulence structure of the flows under consideration and provide an optimum test case to validate the physical modeling of the turbulent structure of VSTOL applications. The results are used to validate numerical calculations of the flow, which are then used to extend the experimental analysis of the entire flowfield.

The present work follows that for single impinging jets presented in Refs. 1 and 2, which have first addressed the question of the lack of available data on impinging jets through a crossflow for low impingement heights. Detailed measurements complemented by a numerical analysis of the flow were presented for velocity ratios between the jet and the crossflow between 30 and 73 and for an impinging height of 5 jet diameters. Previous measurements of the flow properties of twin-jet fountain flows are even more scarce than those of single impinging jets and, again, have only been presented in the absence of crossflow. The most relevant works are reviewed in Ref. 3 and, in general, show that upwash flows are characterized by high turbulence levels and considerably large mixing-layer growth rates compared to conventional turbulent shear flows, e.g., Refs. 4 and 5. However, different interpretations of the measurements have been presented due to the difficulty in measuring complex three-dimensional flows using hot-film and pitot-probe techniques, e.g., Refs. 6 and 7. Only Ref. 3 reports Laser-Doppler Velocimetry (LDV) measurements, including those of shear stress, for twin axisymmetric impinging jets with $S/D = 9$ and 14 and $H/D = 3$ and 5.5, but again the existence of a crossflow was not considered. Those measurements are complemented by the flow visualization analysis of Ref. 8 and show a linear spreading of the

Received June 16, 1988; revision received April 5, 1990.

*Assistant Professor, Mechanical Engineering Department, Av. Rovisco Pais.
†Full Professor, Dean of Engineering, Mechanical Engineering Department, Av. Rovisco Pais.
‡Lecturer, Mechanical Engineering Department, Exhibition Road.

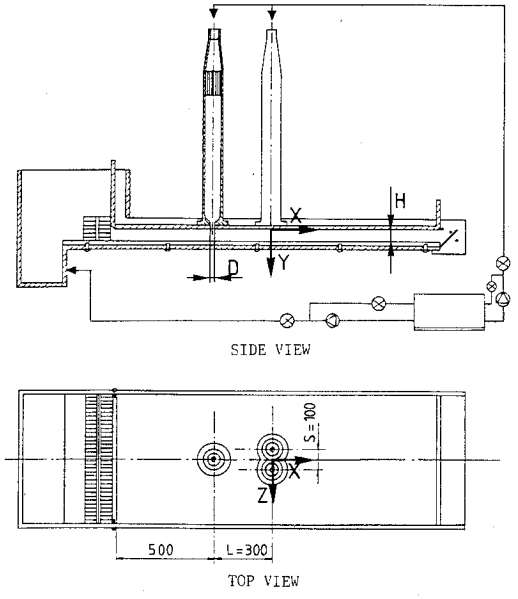

Fig. 1 Diagram of flow configuration (the coordinate system shown is valid for the twin-jet experiments; for the single-jet case the origin of the coordinates is taken at the center of the jet).

fountain with a rate independent of the impingement height. The maximum turbulence intensities were in the range of 50–60%.

Early detailed calculations of impinging jets have only been attempted for single-jet flows, e.g., Refs. 9 and 10, and the numerical analysis presented in this paper follows that of Ref. 2, which has shown that higher-order numerical schemes or very fine meshes have to be used to obtain numerically accurate solutions. This paper presents numerical results for the twin-jet case using the QUICK scheme to evaluate the convective terms and examines the computational method performance in this type of flow based on detailed measurements.

The next section describes the experimental method and gives details of the flow configuration, the laser-Doppler velocimeter, and errors incurred in the measurements. Section III presents and discusses the results, and Section IV summarizes the main findings and conclusions of this work.

II. Flow Configuration, Experimental Technique, and Measurement Procedure

The experiments were carried out in a horizontal water channel 1.50-m long and 0.5-m wide, made of perspex, as shown schematically in Fig. 1. The apparatus was built to allow multijet impingement experiments with variable blockage ratio, H/D, but in the present study single and twin jets of 20-mm exit diameter have been used at a fixed impingement height of 5 jet diameters. The crossflow duct extends $20D$ upstream and $55D$ downstream of the central single-jet entry, which is located at $12.5D$ from each side wall. The twin jets are separated by $5D$ and are located at $10D$ from the nearest side wall. Each jet unit comprises a nozzle with an area contraction ratio of 16 and a settling chamber 0.56-m long, which begins with a 7-deg flow distributor followed by flow straighteners. The facility has a recirculating system whereby both jet and crossflow water is drawn from a discharge tank and pumped to a constant-head tank or supplied to each jet unit via control valves. The uniformity of the crossflow was ensured by straighteners and screens.

The origin of the horizontal X and vertical Y coordinates is taken at the center of the single-jet exit, or between the twin jets, in the upper wall of the tunnel: X is positive in the crossflow direction, and Y is positive vertically downward, as shown in Fig. 1.

The present results were obtained for jet exit mean velocities between 3 and 5.1 m/s, giving rise to Reynolds numbers based on the jet exit conditions between 60,000 and 105,000. The nozzle exit turbulence intensity was measured to be approximately 2%. For twin-jet flows, the two jets were carefully set at equal strengths. The crossflow mean velocities were set to give rise to velocity ratios between the jet and the crossflow of $V_j/U_0 = 30$ for all the flows studied to allow the simulation of practical VSTOL applications. Measurements obtained in the crossflow without the jet have shown that the local turbulence intensity of the crossflow is about 18% and that the wall boundary layer in the jets impingement regions has a uniform thickness around 10 mm.

Flow visualization has been conducted using air bubbles as tracer particles or by introducing a fluorescent dye into the jet flow. Illumination of the flow was achieved by a sheet of light, about 2-mm thick, obtained by spreading a laser beam (argon-ion, 2 W, at 488 nm) with a cylindrical lens.

The experimental equipment and measurement procedure used in this study have been explained in detail in Ref. 1, and only a brief description will be given here. The velocity field was measured by a dual-beam, forward-scatter laser velocimeter, which comprised an argon-ion laser operated at a wavelength of 514.5 nm and a nominal power around 1 W. Sensitivity to the flow direction was provided by light-frequency shifting from acousto-optic modulation (double Bragg cells), a 310-mm focal length transmission lens, and forward-scattered light collected by a 150-mm focal length lens at a magnification of 0.76. The half angle between the beams was 3.48 deg (4.64 deg in air), and the calculated dimensions of the measuring volume at the e^{-2} intensity locations were 2.225 and 0.135 mm. The horizontal U and vertical V mean and turbulent velocity components were determined by a purpose built frequency counter interfaced with a microprocessor, as described by Ref. 11. The fluctuating velocity components were also used, together with those at 45 deg, to compute the local shear stress distribution $\overline{u'v'}$, as in Ref. 12. Measurements were obtained up to 2 mm from the ground plate, with the transmitting optics inclined at half angle of beam intersection and with the scattered light collected off axis. Results obtained 20 mm from the ground plate with both the on-axis and the off-axis arrangements have shown a close agreement within the precision of the equipment.

Errors incurred in the measurements of velocity by displacement and distortion of the measuring volume due to refraction on the duct walls and the change in refractive index were found to be negligibly small and within the accuracy of the measuring equipment. No corrections were made for sampling bias, and the systematic errors that could have arisen were minimized by using high data rates in relation to the fundamental velocity fluctuation rate, as suggested by Refs. 13 and 14. Nonturbulent Doppler broadening (systematic) errors due to gradients of mean velocity across the measuring volume, e.g., Ref. 12, may affect essentially the variance of the velocity fluctuations, but for the present experimental conditions these errors are sufficiently small for their effect to be neglected. The maximum error is on the order of $10^{-4}V_j^2$ and occurs at the edge of the jet. Transit broadening has been shown by Ref.

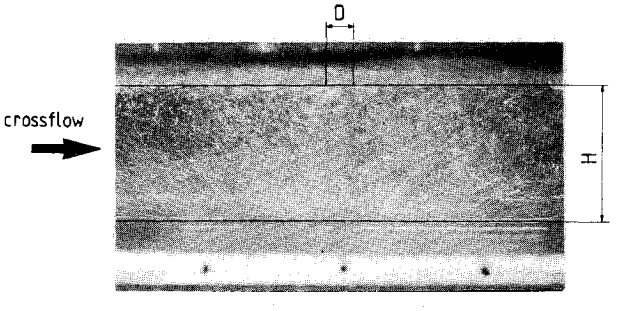

Fig. 2 Visualization of the upwash flow in the central vertical plane for the twin-jet configuration for $Re_j = 105{,}000$, $H/D = 5$, $S/D = 5$, and $V_j/U_0 = 30$.

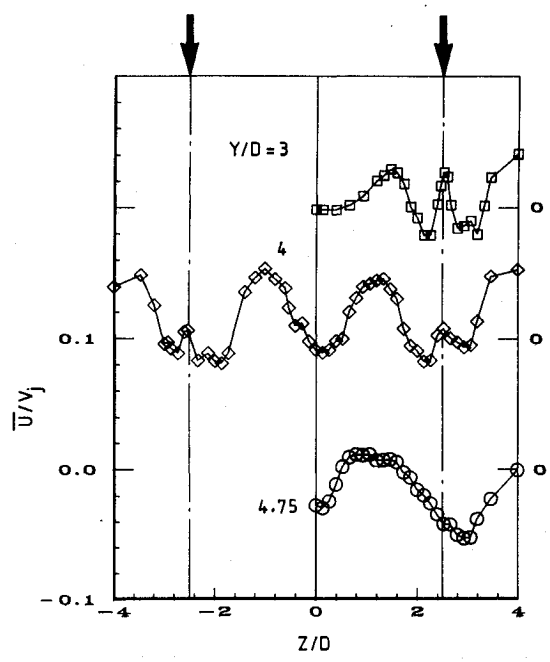

a) Mean horizontal velocity $\bar{U}/V_j$

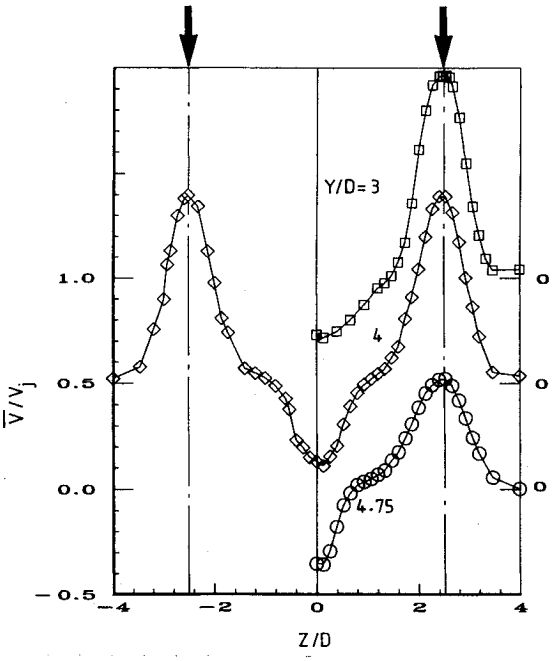

b) Mean vertical velocity $\bar{V}/V_j$

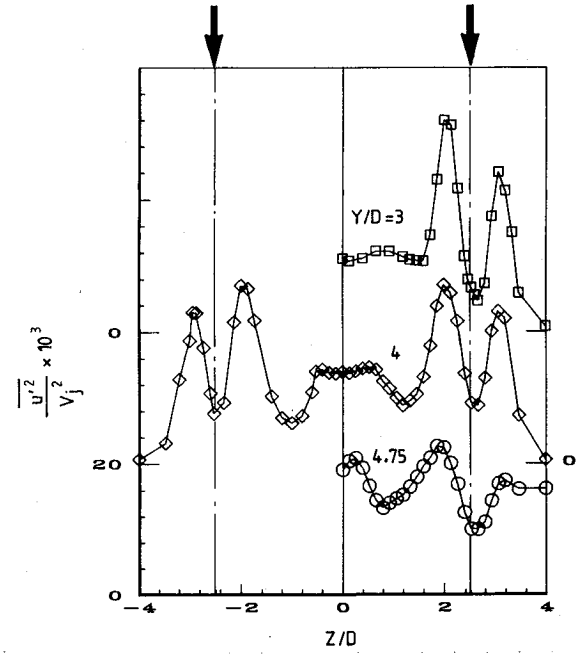

c) Variance of horizontal velocity fluctuations $\overline{u'^2}/V_j^2 \times 10^3$

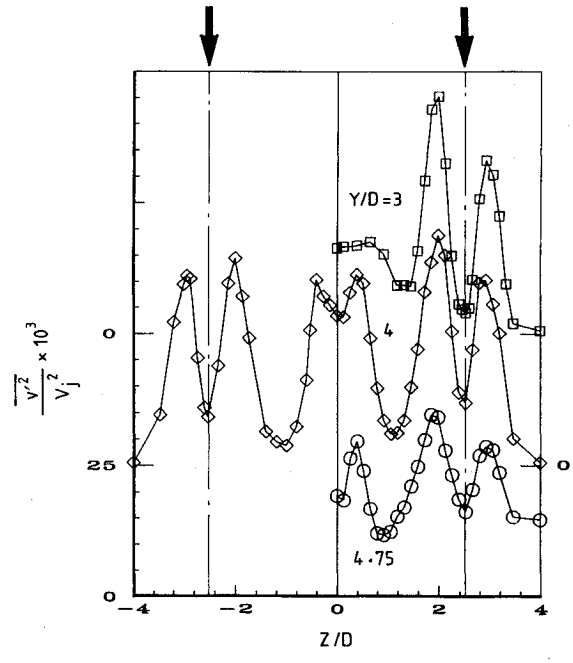

d) Variance of vertical velocity fluctuations $\overline{u'^2}/V_j^2 \times 10^3$

Fig. 3 Horizontal profiles of velocity characteristics for twin-jet flow in the transversal vertical plane crossing the center of the jets for Re_j = 105,000, V_j/U_0 = 30, H/D = 5, and S/D = 5.

15 to be the principal source of error in laser velocimetry; for the present optical configuration, the related signal-to-noise ratio is about 69, and the maximum error in the variance of the velocity fluctuations is on the order of $2 \times 10^{-3} V_j^2$.

The number of individual velocity values used in the experiments to form the averages was always above 10,000. As a result, the largest statistical (random) errors were 1.5 and 3%, respectively, for the mean and variance values, according to the analysis referred to in Ref. 16 for a 95% confidence interval.

III. Results and Discussion

The following paragraphs present and discuss the results under two headings: the first considers flow visualization and selected laser-Doppler measurements of twin-jet flows from a more complete set of results; the second compares experimental results with numerical predictions obtained with a two-equation turbulence model and the QUICK scheme for single- and twin-jet flows and presents a numerical analysis of the fountain flow.

A. Experiments in Twin-Jet Flows

Extensive flow visualization studies were conducted for a range of single- and twin-jet flow conditions, and here typical results are presented and discussed for the flow configuration characterized by Re_j = 105,000, V_j/U_0 = 30, H/D = 5, and S/D = 5, which provides the basic benchmark data for twin-jet flows. The results have shown for each jet a pattern similar

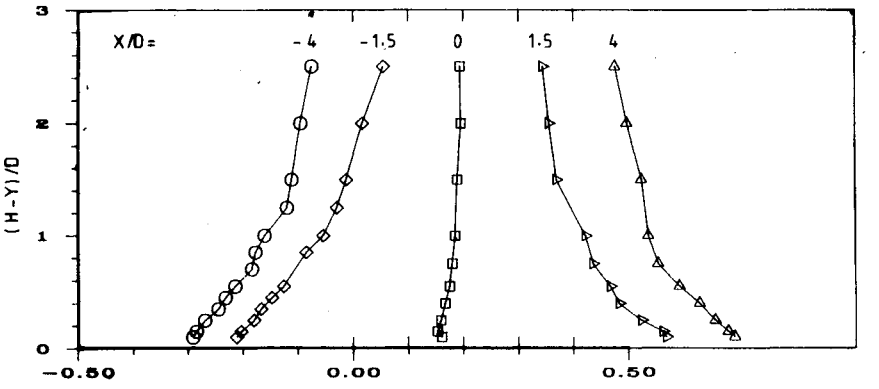

a) Mean horizontal velocity $\tilde{U}/V_j$

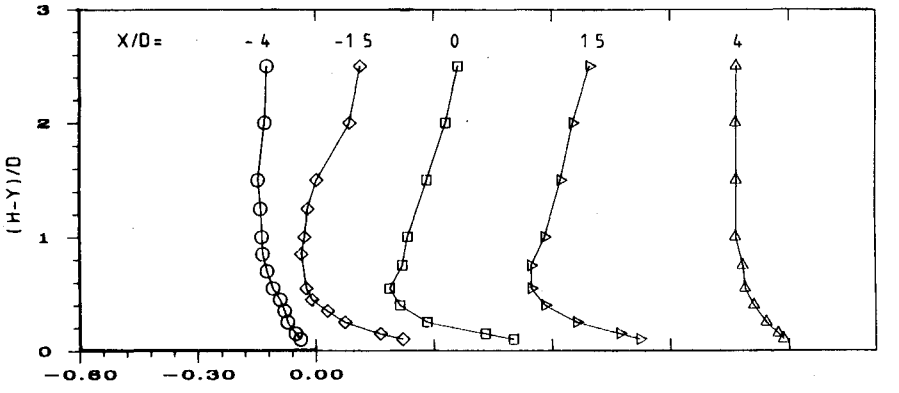

b) Mean vertical velocity, $\tilde{V}/V_j$

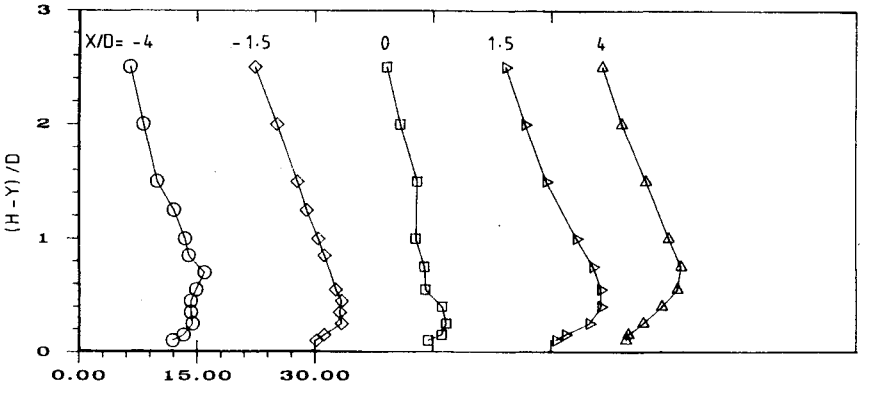

c) Variance of horizontal velocity fluctuations $\overline{u'^2}/V_j^2 \times 10^3$

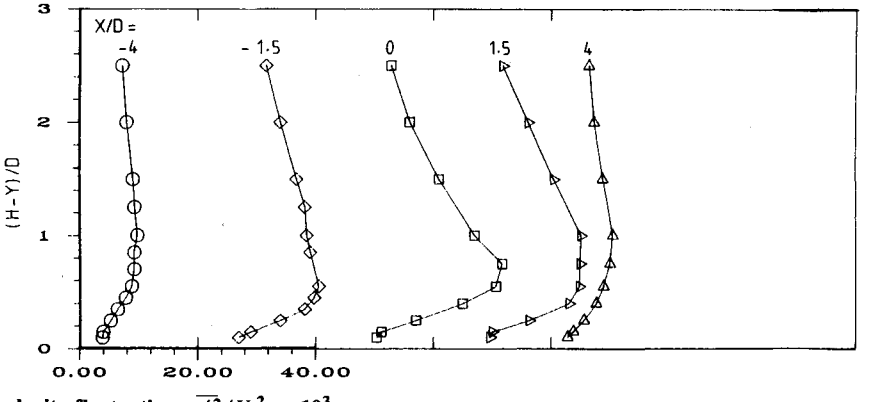

d) Variance of vertical velocity fluctuations $\overline{v'^2}/V_j^2 \times 10^3$

(Continued next page)

Fig. 4 Vertical profiles of mean and turbulent velocity characteristics for twin jets in the vertical plane of symmetry (central plane between the two jets) for Re_j = 105,000, V_j/U_0 = 30, H/D = 5, and S/D = 5.

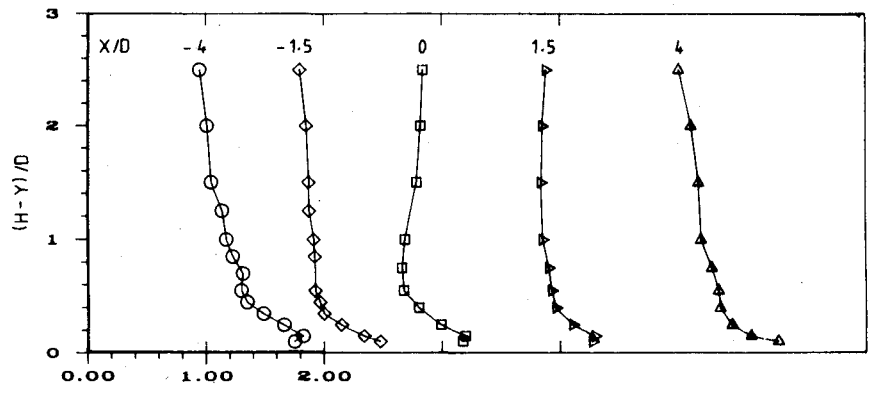

e) Distribution of the relative magnitude of the normal stresses $\sqrt{\overline{u'^2}}/\sqrt{\overline{v'^2}}$

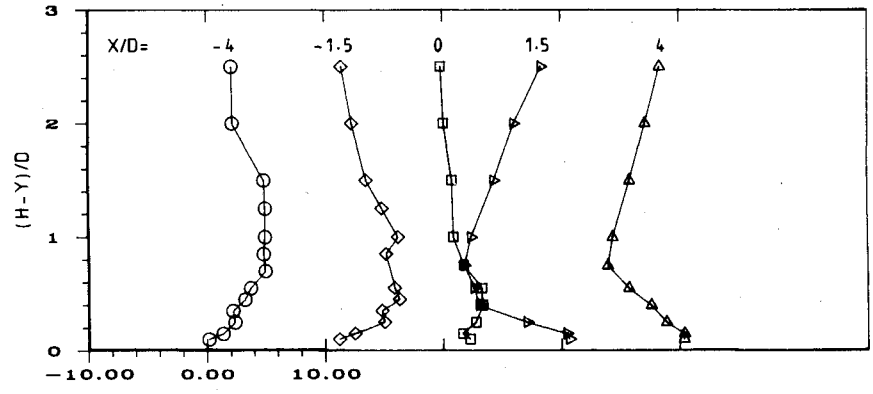

f) Reynolds shear stress $\overline{u'v'}/V_j^2 \times 10^3$

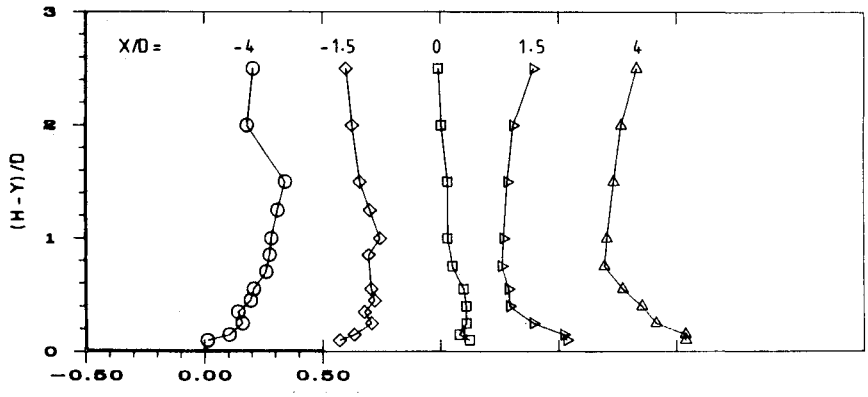

g) Structure parameter $\overline{u'v'}/k$, where $k = 3/4(\overline{u'^2} + \overline{v'^2})$

(Figure 4 continued from previous page.)

to that presented by Ref. 1 for a single impinging jet, comprising an initial potential-core jet region and an impingement region characterized by considerable deflection of the jet. The jet becomes almost parallel to the ground plate and originates a recirculating flow region far upstream of the impinging jet and an upwash flow equidistant from the two impinging jets due to the collision of the two radial wall jets. Figure 2 identifies the upwash in the vertical plane of symmetry, which contains a stagnation line, and shows that the upwash directions in this plane are asymmetric because upstream of the jets, i.e., for $X<0$, the crossflow increases the inclination of the upwash with respect to the ground plane.

Visualization of the flow in the transversal plane containing the center of the two jets has shown that the fountain behaves independently of the main jets. A considerable entrainment of surrounding fluid into the jets and fountain was observed in a way similar to that described in Ref. 8. Visualization studies have also shown that lateral-wall effects do not disturb the fountain upwash flow and, in general, do not affect the conclusions to be drawn from this work. It should be recalled that one of the main purposes of the present experiments is to validate computer codes, which have to assume lateral boundary conditions similar to those of the experiments.

Figures 3 and 4 show sample laser-Doppler measurements of mean and turbulent velocities obtained in the vertical plane crossing the center of the jets and in the vertical plane of symmetry. The results quantify the earlier description of the flow and are analyzed in the following paragraphs.

Figure 3 shows horizontal transversal profiles of axial U and vertical V mean velocity components in the vicinity of the ground plane, i.e., $Y/D > 3$, and quantifies the development of the impinging jets and of the central fountain upwash flow. The measurements, particularly those of the vertical velocity component, clearly identify a centrally located fountain rising from the ground plate without interference from the main jets, as it occurs in practical VSTOL applications. This shows that

the interjet spacing S used in the present experiments is large enough to avoid a sensible deflection of the jets perpendicular to the crossflow. The symmetry of the flow about the central plane between the two jets is also clearly demonstrated in Fig. 3 along the horizontal profiles obtained at $Y/D = 4$. This symmetry in the data distributions indicates the precise matching of the strength of the two jets.

The profiles of the horizontal velocity $\bar{U}$ at $Y/D = 3$ and 4 show peaks along the jet boundaries, which are considerably smaller in magnitude (about $0.4\% V_j$) and may be associated with the transversal recirculatory flows originated by the central and lateral collisions of the wall jets. It should be noted that measurements obtained 2 mm downstream of the jet exit have established precise boundary conditions typical of a potential core jet flow with zero mean horizontal velocities. Based on the detailed measurements of Ref. 2 for single impinging jets for $V_j/U_0 = 30$, it is observed that the influence of the ground plate on the jet flows and the impinging region extend to about $3D$ and $1D$ above the plate, respectively.

The deflection of the impinging jets by the crossflow is here identified close to the ground plate, i.e., $Y/D = 4.75$, by the negative values of the mean horizontal velocity $\bar{U}$ at the geometrical axis of the jet, i.e., $Z/D = 2.5$. The negative values of $\bar{U}$ at $Z = 0$ are a consequence of the longitudinal (i.e., along X direction) asymmetry of the fountain flow discussed above and indicates that the central stagnation point is displaced downstream by the crossflow. These features of the mean flowfield can be readily analyzed by the vertical profiles of the mean axial velocity, shown in Fig. 4a: the values at $X = 0$ are negative along the full profile and, in particular, the profiles at $X/D = \pm 1.5$ are asymmetric with increased absolute magnitudes for $X<0$.

Analysis of the upwash flow shows that along any horizontal profile in the central plane of symmetry, the mean axial velocities increase in absolute magnitude at least up to $X/D = \pm 2.7$ and then decay with increased rates closer to the ground plate. The vertical velocities show maximum upward values around the central stagnation zone and then decay monotonically to zero with X. At $X/D = 8$, the maximum upward vertical velocities increase with the distance to the ground plate and are below $0.08 V_j$. In agreement with the proceeding qualitative analysis, the distributions of the mean velocity components are asymmetric with respect to $X = 0$, with higher upward vertical velocities upstream of the jets. For example, at $X/D = -4$, the inclination of the mean velocity vector reaches values three times larger than that at $X/D = +4$.

Figures 3c, 3d, 4c, and 4d show horizontal and vertical profiles of the normal stresses $\overline{u'^2}$ and $\overline{v'^2}$ and show two regions of intense velocity fluctuations, namely the shear layer surrounding the impinging jets and the fountain upwash flow, with maximum values similar to those found by Ref. 3 in the absence of crossflow. Based on the previous measurements for single impinging jets in Ref. 2, a third region of high velocity fluctuations occur around the two impingement zones. These three regions are characterized by the highest mean velocity gradients and are associated with near-Gaussian velocity probability distributions, suggesting the absence of discrete frequency oscillations. The development of the horizontal profiles of Figs. 3c and 3d quantify the turbulent diffusion along the jets: the peaks of the normal stresses spread along the jet, and the minima in the center of the jets increase in magnitude as Y increases. The consistent asymmetry of the distributions of the normal stresses along the jets is probably associated with convection from the highly turbulent upwash flow, which exhibits maximum fluctuating values close to the ground plate.

The flow is anisotropic in that, with exception of the initial potential core, $\overline{v'^2}$ is largest around the jet and in the upwash flow, with $\sqrt{\overline{u'^2}}/\sqrt{\overline{v'^2}} \geq 0.6$ whereas, following Ref. 2, $\overline{u'^2}$ is largest along the wall jets, with $\sqrt{\overline{u'^2}}/\sqrt{\overline{v'^2}} \leq 1.4$. The anisotropy of the upwash flow is particularly observed along the vertical plane of symmetry; see Fig. 4e. Close to the ground plate, $\overline{u'^2}$ is largest, with $\sqrt{\overline{u'^2}}/\sqrt{\overline{v'^2}} = 1.8$ at $X/D = \pm 4$ whereas, away from the ground plate and downstream of $X/D = +4$, $\overline{v'^2}$ is largest with $\sqrt{\overline{u'^2}}/\sqrt{\overline{v'^2}} = 0.65$ at $X/D = 0$.

Figure 4f shows profiles of Reynolds shear stress along the central vertical plane, which are consistent with the longitudinal asymmetry of the upwash flow and, in general, with the direction of the mean flow. For $X<0$, the shear stress is positive because faster moving elements of upward fluid ($v'<0$) tend to move far upstream ($u'<0$). Similarly, the shear stress downstream of the jets, i.e. $X>0$, is negative because there the upward movement of fluid particles is associated with positive axial velocity fluctuations.

The distribution of shear stress away from the fountain upwash flow may be analyzed on the basis of the results of Ref. 1. The impinging jets and the radial wall jets are dominated by the mean strains $\partial\bar{U}/\partial Y$ and $\partial\bar{V}/\partial X$, respectively, and the sign of the shear stress is related to that of each shear strain in accordance with a turbulent viscosity hypothesis. Around the impinging point, the values of the mean strains have the same order of magnitude[3] because the flow is subject to strong stabilizing curvature,[17,18] and the gradient diffusion approximation does not represent the flow. The maximum values of the correlation coefficient of shear stress occur along the impinging wall jets and are about 0.55 and, therefore, close to the values found in undisturbed shear layers. In the impingement region, the correlation coefficient is below 0.2.

The present results extend those analyses to the fountain upwash flow, which is again subject to strong curvature effects and influenced not only by the competing magnitudes of the mean strains $\partial\bar{U}/\partial Y$ and $\partial\bar{V}/\partial X$ but also by extra rates of strain. The shear stress around the stagnation point is close to zero in zones of zero shear strain, and the high turbulence levels measured there may be explained by the interaction of normal stresses and normal strains. In general, the results reported here suggest that the calculation of the turbulent struc-

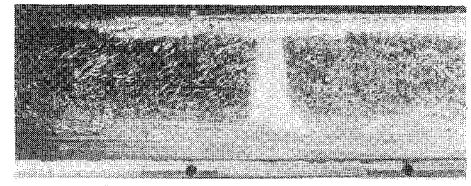

a) Flow visualization using air bubbles as tracer particles

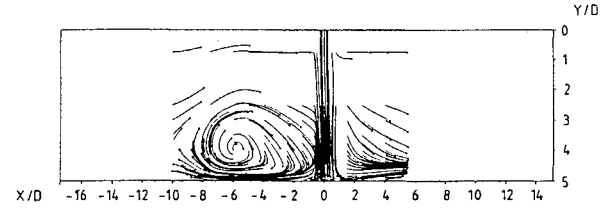

b) Measured streaklines over 0.2 s

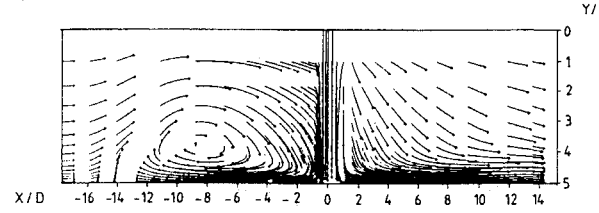

c) Calculated streaklines over 0.2 s using the higher-order QUICK numerical scheme together with the k - ϵ model of turbulence in a mesh of 30 × 17 × 17

Fig. 5 Experimental and numerical analysis of the single-jet flow in the vertical plane of symmetry for $Re_j = 60{,}000$, $V_j/U_0 = 30$, and $H/D = 5$.

ture of the upwash flow requires consideration of the individual stresses.

The nature of the turbulent structure of the upwash flow can be readily analyzed from the values of typical structure parameters. The maximum absolute values of the correlation coefficient of shear stress in the central vertical plane occur at the location of maximum axial normal stress and are equal to 0.5 and, therefore, similar to those reported by Ref. 3 in the absence of crossflow. The profiles of the ratio of shear stress upon the turbulent kinetic energy, $\overline{u'v'}/k$ in Fig. 4g, show maximum values equal to 0.3, similar to those found in undisturbed shear flows.[19]

B. Numerical Simulation of Single- and Twin-Jet Flows

The detailed nature of the mean and fluctuating velocity measurements make the aforementioned data eminently suitable for validation of numerical models of the flow.

Simulations consist of finite-difference solutions of the incompressible steady-state form of the Navier-Stokes equations obtained with the method used in Ref. 2. Turbulence is modeled with the standard "k - ϵ" model using the constants indicated by Ref. 2, which have been used in a wide range of turbulent shear flows providing good agreement with experiments.[20]

Reference 2 did report some preliminary calculations of single impinging jet flows, using the k - ϵ turbulence model together with the first-order hybrid numerical scheme implemented in a mesh of 30 × 17 × 17 nodes, and found it necessary to adopt a higher-order descretization scheme for the convective terms, or fine meshes, to obtain numerically accurate solutions. Following the calculations in Ref. 2, Ref. 21 compares predicted profiles of $\bar{U}$, $\bar{V}$, k, and $\overline{u'v'}$ obtained with the hybrid and the QUICK scheme and different meshes. The grid independent solution obtained with the QUICK scheme and 30 × 17 × 17 nodes gives good agreement with the measurements and is equivalent to the 60 × 34 × 34 hybrid solution. However, in the immediate vicinity of the impinging point, the sign of the shear stress $\overline{u'v'}$ is wrong because, as shown by Ref. 2, the gradient hypothesis does not represent the flow in this region. Figure 5 shows the flowfield of a single impinging jet visualized in the vertical plane of symmetry and compares particle tracks or streaklines of the measured and predicted velocity fields in the same plane. The figure allows a clear visualization of the impinging jet and the upstream scarf vortex and shows that the QUICK scheme implemented in a relatively coarse mesh may predict the gross features of the flow.

The numerical method used by Refs. 2 and 21, which allows good agreement with the measurements of the mean velocity field, is now used to evaluate the ability of the k-ϵ model to simulate the previously described twin-jet flows. As in the case of single impinging jets, the computational domain has six boundaries where the dependent values are specified: an inlet and outlet plane, a symmetry plane, and solid walls at the top, bottom, and side of the channel. At the inlet boundary, uniform profiles of all dependent variables are specified from the experimental results, and its location is sufficiently far away from the jets so that the details of the boundary conditions have a negligible influence on the results. At the outflow boundary, the gradients of the dependent variables in the axial direction are set to zero. On the symmetry plane, the normal velocity and the normal derivatives of the other variables are set to zero. The wall functions are used on the solid surfaces, assuming that in the near-wall region the velocity profile is given by the log-law (see Ref. 20). The jet exit boundary conditions are also prescribed from the experiments.

The numerical results presented in Figs. 6 and 7 were obtained using a grid of 16 × 27 × 23 nodes with a nonuniform spacing to get finer spacing near the jet and upwash. A grid of 20 × 35 × 30 nodes was also used to investigate the grid dependency of the solution. The effect of this grid refinement is illustrated in Fig. 8, which presents measured and calculated

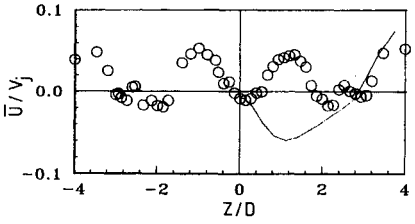

a) Mean horizontal velocity $\bar{U}/V_j$

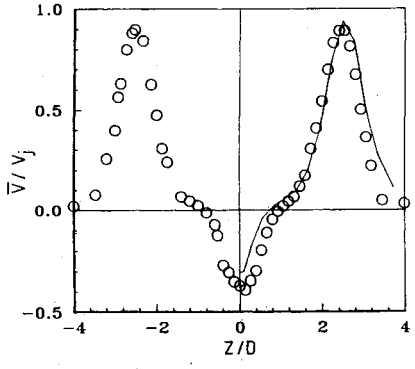

b) Mean vertical velocity $\bar{V}/V_j$

Fig. 6 Measured and calculated (QUICK scheme with 23 × 16 × 27 nodes) horizontal profiles of velocity characteristics for twin-jet flow in the vertical plane crossing the center of the jets at Y/D = 4, Re_j = 105,000, V_j/U_0 = 30, H/D = 5, and S/D = 5: measurements: o; predictions: —.

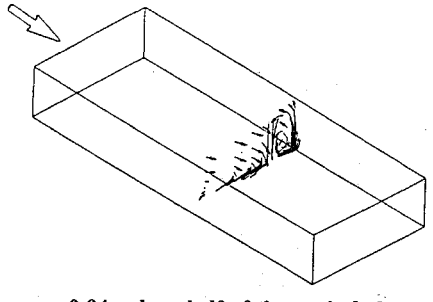

a) Streaklines over 0.04 s along half of the vertical plane crossing the center of the jets

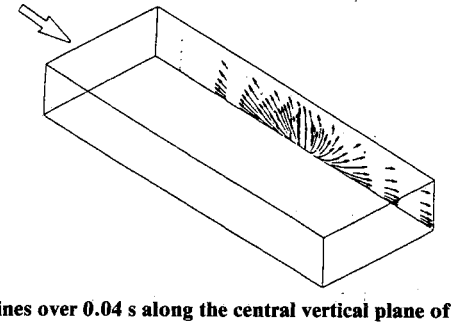

b) Streaklines over 0.04 s along the central vertical plane of symmetry

Fig. 7 Numerical analysis of twin-jet flow using the QUICK scheme with a mesh of 23 × 16 × 27 for Re_j = 105,000, V_j/U_0 = 30, H/D = 5, and S/D = 5.

horizontal profiles in the vertical plane of symmetry at Y/D = 4. The agreement with the measurements is not improved with the finer mesh, which gives similar results to those obtained with the 16 × 27 × 23 mesh, and therefore the grid refinement is not worth the extra computational effort involved.

Figure 6 shows measured and calculated horizontal profiles of velocity characteristics in the vertical plane crossing the center of the two jets (X = 0). The numerical results show that the gross features of the mean flowfield and in particular the impinging jet are well predicted. Nevertheless, the sign of the predicted mean axial velocities at Y/D = 4 is wrong due to the

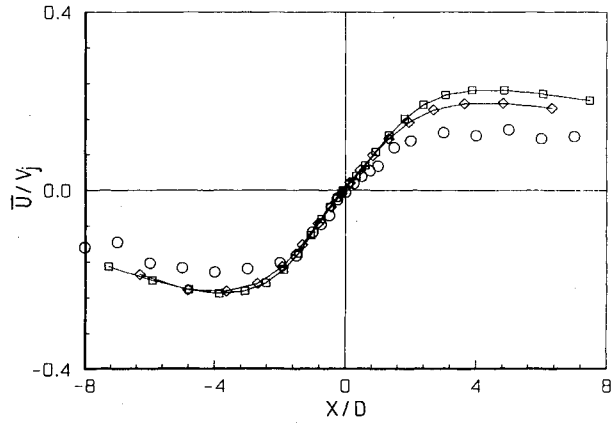

Fig. 8 Measured and calculated horizontal profiles of $\bar{U}/V_j$ in the vertical plane of symmetry at $Y/D = 4$: measurements: ○; predictions: ◇ 16 × 27 × 23 mesh, □ 20 × 35 × 30 mesh.

failure in predicting the exact location of the central stagnation point, which is at $X/D = +0.1$, instead of the calculated value of $X/D = -0.1$.

The preceding paragraphs have considered the validation procedure of the numerical method used to simulate the twin-jet flows under consideration. We now turn to the numerical analysis of the upwash flow. Figures 7a and 7b show predicted streaklines in the vertical plane crossing the center of the two jets and in the central plane of symmetry. The figures allow a clear visualization of one impinging jet and of the fountain, which follow the three-dimensional flow patterns described in the previous section. Each impinging jet is considerably deflected by the ground plate, and the consequent inner wall jets are further subject to strong curvature at the fountain upwash flow.

IV. Conclusions

Laser-Doppler measurements have provided information about the mean and turbulent velocity characteristics of the flows created by a single round jet impinging on a ground plate through a confined crossflow for $H/D = 5$ and $V_j/U_0 = 30$ and by axisymmetric twin jets positioned side by side with a spacing of $5D$ with fountain formation. The experimental results were used to validate numerical calculations of the flow based on the solution of the finite-difference form of the fully tridimensional Navier-Stokes equations, incorporating the turbulence viscosity concept. The following is a summary of the more important findings and conclusions of this work:

1) The experiments have shown large penetration of the impinging jets, which exhibit a similar pattern for single- and twin-jet configurations. For the latter, the fountain upwash flow formed by collision of the radial wall jets is deflected by the crossflow.

2) The shear layer surrounding the jets, the impingement region, and the fountain are zones of intense velocity fluctuations. The latter are dominated by strong curvature effects, and the calculation of their turbulent structure requires consideration of the individual stresses.

3) Grid independent numerical calculations of the single- and twin-jet flows with the QUICK scheme and the k-ϵ turbulence model are shown to represent adequately the gross features of the flows. The method fails to predict the turbulent structure of the impingement zones and the fountain flow because of the inapplicability of the turbulent viscosity hypothesis.

Acknowledgments

This work was a collaboration between the CTAMFUTL-INIC (Centro de Termodinamica Aplicada e Mecanica de Fluidos da Universidade Tecnica de Lisboa) and the Fluids Section of the Imperial College of Science and Technology.

References

[1]Barata, J. M. M., Durão, D. F. G., Heitor, M. V., and McGuirk, J. J., " Experimental and Numerical Study on the Aerodynamics of Jets in Ground Effect," Tenth Symposium on Turbulence, Univ. of Missouri-Rolla, MO, Sept. 1986; also, *Experiments in Fluids* (to be published).

[2]Barata, J. M. M., Durão, D. F. G., Heitor, M. V., and McGuirk, J. J., "The Turbulent Characteristics of a Single Impinging Jet Through a Crossflow," Sixth Symposium on Turbulent Shear Flows, Toulouse, France, 1988.

[3]Saripalli, K. R., "Laser Doppler Velocimeter Measurements in 3D Impinging Twin-Jet Fountain Flows," *Turbulent Shear Flows*, Vol. 5, edited by F. Durst et al., Springer-Verlag, Berlin 1987, pp. 147–168.

[4]Gilbert, B. L., "Detailed Turbulence Measurements in a Two Dimensional Upwash," AIAA Paper 83-1678, July 1983.

[5]Kind, R. J., and Suthanthiran, K., "The Interaction of Two Opposing Plane Turbulent Wall Jets," AIAA Paper 72-211, Jan. 1980.

[6]Jenkins, R. C., and Hill, W. G., Jr., "Investigation of VTOL Upwash Flows Formed by Two Impinging Jets," Grumman Research Dept. Rept. RE-548, Bethpage, NY, Nov. 1977.

[7]Kotansky, D. R., and Glaze, L. W., "The Effects of Ground Wall-Jet Characteristics on Fountain Upwash Flow Formation and Development, Office of Naval Research, Rept. ONR-CR212-216-1F, 1980.

[8]Saripalli, K. R., "Visualization of Multijet Impingement Flow," *AIAA Journal*, Vol. 21, No. 4, 1983, pp. 483–484.

[9]Jones, W. P., and McGuirk, J. J., "Computation of a Round Turbulent Jet Discharging Into a Confined Crossflow," *Turbulent Shear Flows*, edited by F. Durst, et al., Springer-Verlag, Berlin, Vol. 2, 1980, pp. 233–245.

[10]Childs, R. E., and Nixon, D., "Simulation of Impinging Turbulent Jets," AIAA Paper 85-0047, Jan. 1985.

[11]Heitor, M. V., Laker, J. R., Taylor, A. M. K. P., and Vafidis, C., "Introduction Manual for the FS Model 2 Doppler-Frequency Counter," Imperial College, London, Mechanical Engineering Dept. Rept. FS/84/10, 1984.

[12]Durst, F., Melling, A., and Whitelaw, J. H., *Principles and Practice of Laser-Doppler Anemometry*, 2nd ed., Academic, New York, 1981.

[13]Dimotakis, F., "Single Scattering Particle Laser-Doppler Measurements of Turbulence," AGARD-CP-13, Paper 10.7, 1978.

[14]Erdmann, J. C., and Tropea, C. D., "Turbulence-Induced Statistical Bias in Laser Anemometry," *Proceedings of the 7th Biennal Symposium on Turbulence*, 1981.

[15]Zhang, Z., and Wen, J., "On Principal Noise of the Laser Doppler Velocimeter," *Experiments in Fluids*, Vol. 5, 1987, pp. 193–196.

[16]Yanta, W. J., and Smith, R. A., "Measurements of Turbulent-Transport Properties with a Laser-Doppler Velocimeter," AIAA Paper 73-169, 1978.

[17]Bradshaw, P., "Effects of Streamline Curvature on Turbulent Flow," Agardograph 169, 1973.

[18]Castro, I. P., and Bradshaw, P., "The Turbulence Structure of a Highly Curved Mixing Layer," *Journal of Fluid Mechanics*, Vol. 73, 1976, pp. 265–304.

[19]Harsha, P. T., and Lee, S. C., "Correlation Between Turbulent Shear Stress and Turbulent Kinetic Energy," *AIAA Journal*, Vol. 8, 1970, pp. 1508–1510.

[20]Launder, B. E., and Spalding, D. B., "The Numerical Computation of Turbulent Flows," *Computational Methods in Applied Mechanical Engineering*, No. 3, 1974, pp. 269–289.

[21]Barata, J. M. M., Durão, D. F. G., and McGuirk, J. J., "Numerical Study of Single Impinging Jets Through a Crossflow," *Journal of Aircraft*, Vol. 26, No. 11, 1989, pp. 1002–1008.